Stability study of grid-connected photovoltaic system

by

Wasif A. Choudhury (132408)
Md. Fahim Hossain (132430)
Md. Tasbir Zaman Tonmoy (132431)
Sifat Zaman (132433)

A Thesis Submitted to the Academic Faculty in Partial Fulfillment of the Requirements for the Degree of

BACHELOR OF SCIENCE IN ELECTRICAL AND ELECTRONIC ENGINEERING

Department of Electrical and Electronic Engineering
Islamic University of Technology (IUT)
Gazipur, Bangladesh
November 2017

Stability study of grid-connected photovoltaic system

Approved by:

Dr. Ashik Ahmed
Supervisor and Assistant Professor,
Department of Electrical and Electronic Engineering,
Islamic University of Technology (IUT),
Boardbazar, Gazipur-1704.
Date:

Mehedi Hassan Galib
Co-supervisor and Lecturer,
Department of Electrical and Electronic Engineering,
Islamic University of Technology (IUT),
Boardbazar, Gazipur-1704.
Date:

Table of Contents

List of Tables

List of Figures

List of Acronyms

CSP	Concentrated Solar Power
PV	Photovoltaics
CST	Concentrated Solar Thermal
P	Active Power
Q	Reactive Power
Z	Impedance
R	Resistance
X	Reactance
Y	Admittance
L	Inductance
C	Capacitance
δ	Load Angle
φ	Phase
U	Voltage
d	Direct Axis
q	Quadrature Axis
d_c	Duty Cycle
AC	Alternating Current
DC	Direct Current
G	Solar Irradiation
PWM	Pulse Width Modulation
MPP	Maximum Power Point
MPPT	Maximum Power Point Tracking

Acknowledgements

Firstly, we would like to express our thankfulness to Almighty Allah for giving us the ability to complete this work in good health and vigor.

Then we would like to thank our supervisor Dr. Ashik Ahmed for the continuous support of research, for his patience, motivation, enthusiasm and immense knowledge. His guidance helped us in all the time of research and writing of this thesis. We could not have imagined having a better advisor and mentor for our research project.

Our sincere thanks goes to our co-supervisor Mr. Mehedi Hassan Galib for guiding us throughout this project.

And last but not the least we are thankful to our family, friends and well-wishers for their support and encouragement. Without them, it would never have been possible for us to make it this far.

Abstract

This paper investigates the impact of a large photovoltaic (PV) penetration on power system small signal oscillation stability. A comprehensive model of a single-machine infinite-bus power system integrated with a PV power generation power plant is established. Numerical computation of damping torque contribution from the PV power plant is carried out, which is confirmed by the results of calculation of system oscillation model and non-linear simulation. Those results indicate that power system oscillation stability can be affected either positively or negatively. There exists an operational limit of the PV power plant as far as system oscillation stability is concerned. Beyond the operational limit, the PV generation supplies negative damping torque, thus damaging system oscillation stability. Hence for the safe penetration of PV generation into power systems, the operational limit of oscillation stability of the PV power plant must be considered.

Chapter 1

Introduction

This chapter introduces the background to the stability study of grid connected solar PV system. It describes the motivation and objective of studying the topic of solar PV power integration.

1.1 Background

Solar power is the production of electric power by utilizing thermal energy of sunlight rays from the sun. It consists of a solar power source and a converter of the energy from sunlight to electric energy. This power can be independent of a conventional power grid or can be integrated to an existing conventional electricity grid at transmission or distribution level. Solar power is divided into two branches of technology that are popular today. These are Concentrated Solar Power (CSP) and Photovoltaic (PV) solar power systems.

Solar power in form of CSP operates similar to thermal power plants and is sometimes referred to as Concentrated Solar Thermal. It uses reflecting mirrors that reflect sunlight to a common point and heat a fluid that can further drive a turbine to generate electricity. It is an indirect solar power system. In a solar PV power, sunlight is converted to electrical energy directly by using a photovoltaic material (semiconductor material). The sun hits this material and by photovoltaic action in the material, electrical energy is generated. Concentrated Solar Power system operates like conventional thermal power plants and their effects on the grid can be understood by understanding a thermal power plant. Of much interest is the Photovoltaic (PV) solar power system that operates different from conventional generating systems and the effects to an existing transmission or distribution system need to be fully understood before much integration can be made to any distribution or transmission system in power system.

A solar photovoltaic (PV) power system can operate in isolation or connected to a power grid. The system normally consists of a micro power source (solar) and some local loads. Additionally, it can be a solar system without any loads connected but connected to a power grid. When

connected to a grid, the operating conditions of the grid are altered in either a positive or negative way.

There has been rapid increase of grid connected solar PV power in rural, urban and city areas around the globe (e.g. Sweden, Germany, India and some parts of Africa) [1]. This is to enable solar PV Power systems to supply generated power locally and to other places through the existing transmission and distribution power grid. This integration of solar PV power can result in improvements of the grids or can have negative impacts on the steady state system operation parameters.

1.2 Motivation

Small signal stability is defined as the ability of the system to maintain synchronism when it is subjected to small disturbances [2]. In this context, there are two types of instability that can occur: the steady state rotor angle increase due to lack of synchronizing torque and the increasing rotor oscillations due to insufficient damping torque are the two major types of small signal instability [3]. Generator–turbine inertia generally plays a key role in providing synchronizing capability to the synchronous generators whenever a disturbance results in a mismatch between the mechanical power input and the electrical power output of a generator. In a system with high PV penetration, some of the synchronous generators are replaced with PV units. The authors in [4] have proposed a general approach for integration of variable energy resources. The method suggests that for every 3-MW addition of renewable generation to the system, there would be a 2-MW reduction in conventional generator commitment and 1-MW reduction in their dispatch. While the choice of the cited "1/3–2/3 rule" could be quite arbitrary, note that the overall system inertia is decreased, which can lead to potential small signal stability problems. Consequently, with displacing/rescheduling of conventional units as a result of the addition of PV generation, it is advantageous to determine if a particular generator's inertia has significant impact on a particular inertial oscillation mode. This could be determined by performing sensitivity analysis with respect to generator inertia and performing rescheduling using the sensitivity to inertia as a constraint.

1.3 Aim

The objective of this paper is to examine the effect of operation of PV generation jointly with that of conventional generator and transmission system on power system small signal oscillation stability. The paper beings with the establishment of a comprehensive model of a single-machine infinite-bus power system integrated with a PV power generation plant. Then an example single-machine infinite-bus power system integrated with a PV power plant is presented. Results of numerical computation and non-linear simulation at different operating conditions are given when the load conditions of conventional power generation and levels of mixture of conventional and FC generation change. Results from the example power system indicate that power system oscillation stability can be affected either positively or negatively. There exists an operational limit of the PV power plant as far as system oscillation stability is concerned. Beyond the operational limit, the PV generation supplies negative damping torque, thus damaging system oscillation stability. Hence for the safe penetration of PV generation into power systems, the operational limit of oscillation stability of the PV power plant must be considered.

Chapter 2

Literature Study

This chapter introduces the concepts of literature that is in line to the subject of integrating solar PV power to an existing grid and stability of that combined system. It describes the concept of solar PV power, PV penetration and small signal stability.

2.1 Solar Power

Solar power, an important renewable power, has been on the increase in most parts of the world in terms of installations [1]. This is as a result of abundant sunlight shining on the earth from the sun every year and making conversion of this source to usable sustainable electric power a top priority for most developed and developing countries. In Europe, Germany has taken a major leading role in the installation and integration of solar power while Sweden lags behind. Various technologies of solar power harnessing can be used, but today the concentration has been more on two technologies. A technology utilizing the principle of thermal power plants called concentrated solar power (CSP) or solar thermal (CST) is one of them [5]. The other technology uses the photovoltaic effect and is known as solar photovoltaic (PV) power. In a concentrated solar power (CSP), thermal energy is reflected to a receiver and makes the point on the receiver concentrated with thermal energy. The concentrated thermal energy is used to heat a fluid that drives a turbine that is coupled to an alternator. The alternator generates electric power. A CSP system operates and behaves like a conventional thermal power plant [5]. In a solar PV system, a solar cell is used to convert energy (e.g. thermal and radiant) in sunlight into a direct current (dc) power [6]. Figure 2.1 shows a simple process of conversion from sunlight to electric power.

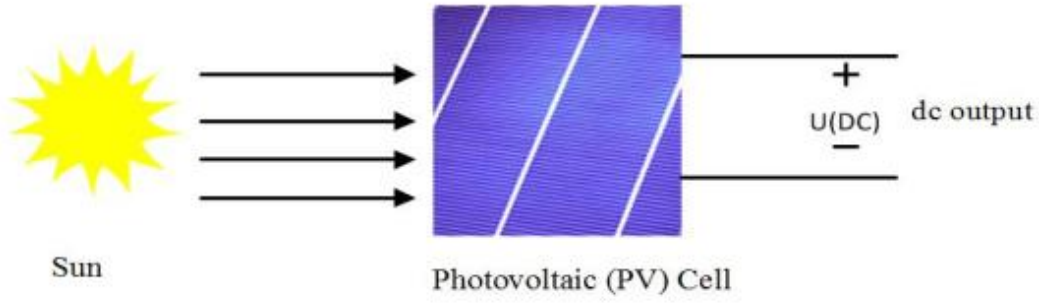

Figure 2.1: Photovoltaic (PV) Cell System [6]

The material used in this solar cell is silicon and semi-conductive in nature. The materials in use today for majority of solar cells are mono-crystalline, poly-crystalline and amorphous silicon [7]. The current and voltage from a single cell is very small. For higher voltage and current, the cells are connected in series to increase the output voltage and in parallel to increase the output current. A combination of cells make up a solar PV module and a combination of modules make up a PV array for high voltage, current and power output. A solar PV array consists of series-parallel arrangement of modules. Since a direct current power is generated, it can be used in two ways. The first way is to have a grid of dc loads that are able to utilize the generated dc power. The second way is to connect power conditioning devices (power electronics converters) to transform generated dc power to alternating current (ac) power. This is because most of the electrical loads today operate with alternating current (ac) power. Figure 2.2 shows a complete arrangement of a solar PV array with power conditioning devices for conversion to alternating current output power.

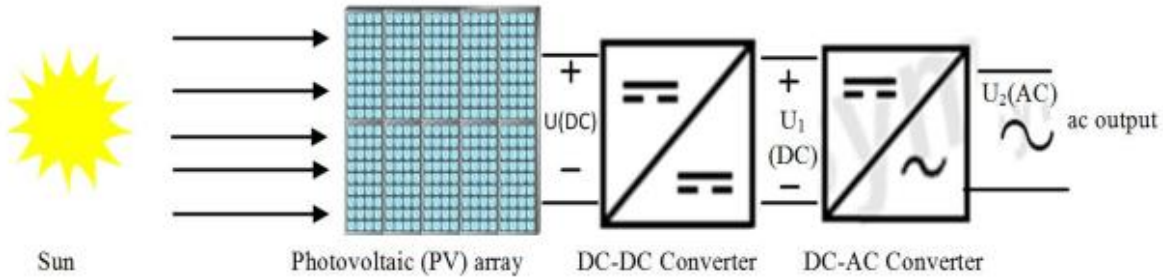

Figure 2.2: Typical Complete Solar PV System [8]

The output dc voltage (U) and current varies with irradiation reaching the array and temperature changes. The DC-DC converter ensures that the dc (U1) fed to the dc-ac inverter is stable. The inverter converts DC to AC (U2) which can be either single phase or three phases depending on the requirement. For integration to a grid, cables, filter circuits and a transformer are added at the output of the inverter.

2.1.1 Photovoltaic (PV) Solar Cell Theory

A PV solar cell made of silicon, a semiconductor, has properties similar to a p-n junction diode. It has a p-region and an n-region. The p-region has more holes (+ positive particles) than electrons (- negative particles) and the n-region has the opposite of the p-region [9]. Because of this, the natural movement of holes and electrons in the material create an electric field in the p-n junction material. When a photon from sun's radiation hits a p-n junction and an electron is dislodged across the depletion region in the n-side, it is accelerated by the field and pushed towards the n-region while the corresponding hole is pushed towards the p-region. Figure 2.3 shows an arrangement of a p-n junction and the depletion layer with the created electric field.

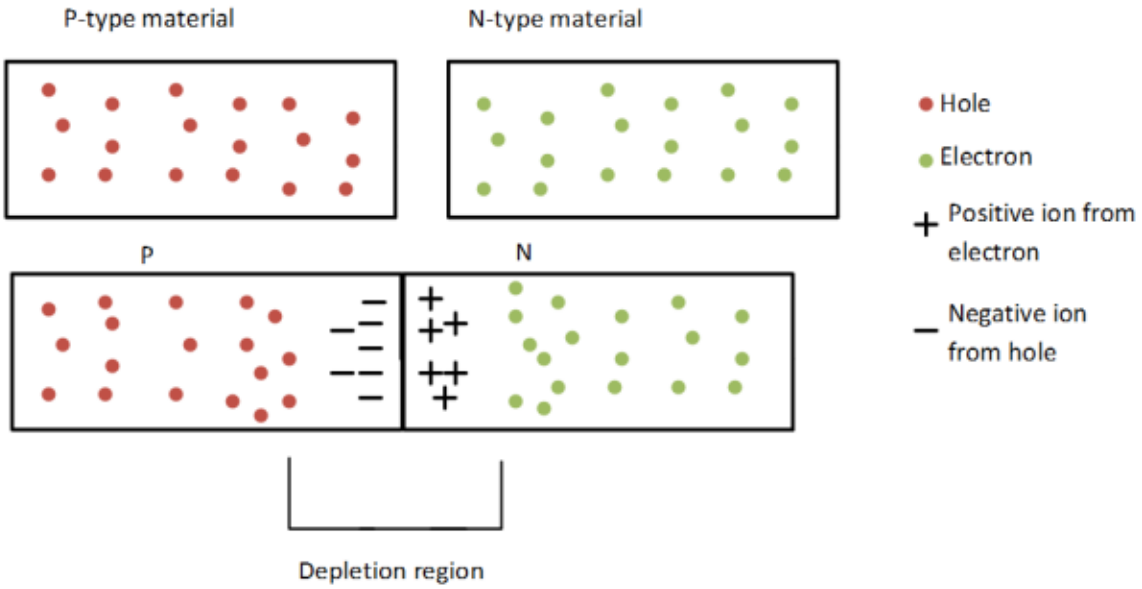

Figure 2.3: P-N Junction [9], [10], [11]

As shown in Figure 2.3, more dislodgement of holes and electrons by photons from sun's radiation creates a field in the depletion region and a difference in polarity of the P and N regions. If an external circuit is connected to the P and N regions, there is poised to be recombination and a dc electric current would flow.

2.1.2 Solar PV Cell Circuit Representation

A solar PV cell for analysis is presented in Figure 2.4 as a constant current source which is a function of the sun's radiation, a diode with a series resistance (RS) and a parallel resistance (RP).

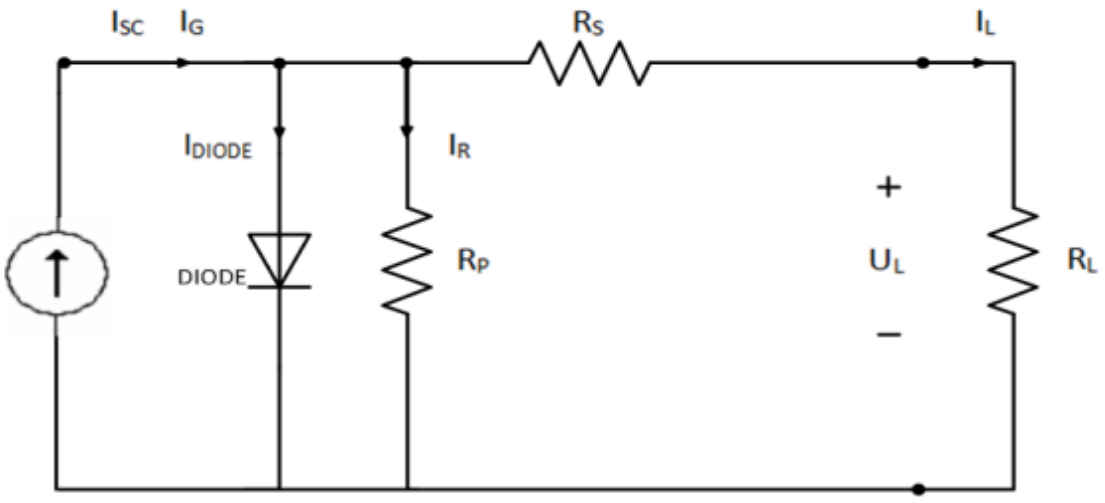

Figure 2.4: Solar Cell Circuit Model

When there is no solar radiation (G) from the sun, there is a backward current that flows in a p-n junction called a dark current (Io). When there is radiation from the sun, the current IG is produced by the cell and with a load connected; an electric current can flow and be measured in the external circuit (IL). The resistor, RL, is depicting a load connected to the solar cell, which for now assumed resistive, and the voltage UL is the open circuit voltage that can be

recorded when there is no load connected. The current IG is the maximum current that the cell can produce at a particular solar radiation (G) and ISC is a current that can be produced with shorted cell terminals. The output current IL is the current that can be recorded for a particular load and solar irradiation (G). This is shown as a block model with power as the output in Figure 2.5.

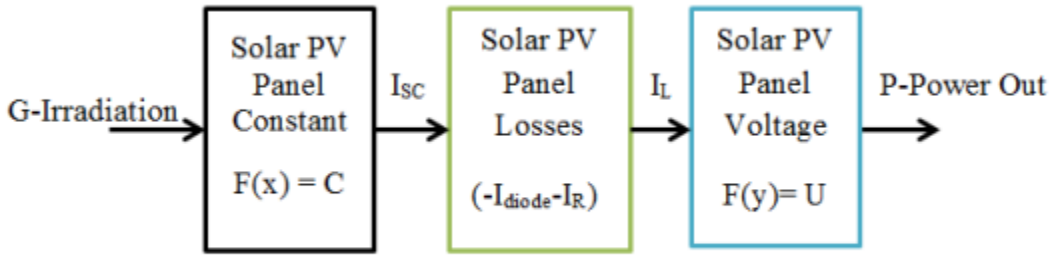

Figure 2.5: Solar PV Block Model Representation

The current for a diode representation is given by the following equation [9]:

$$I_{DIODE} = I_O(e^{\frac{qU_{DIODE}}{n.k.T}} - 1)$$

where, I_{DIODE} is diode current, k is the Boltzmann's constant (8.62 x 10-5 eV/K), q is the number of electron charges per electron, U_{DIODE} is the diode voltage, n: a material constant between 1 and 2, T is the diode temperature in kelvin (K) and I0 is the dark current.

By using Figure 2.4 and Figure 2.5, the output current (IL) can be calculated as follows:

$$I_L = I_{SC} - I_{DIODE} - I_R$$

The short current ISC at a particular solar radiation G in equation (2.2) is given by equation (2.3):

$$I_{SC} = C.G$$

where G is the solar irradiation and C is a constant for the solar cell.

By varying the irradiation on the solar cell and measuring the voltage and current output, a current-voltage (I-U) characteristic of the solar cell can be plotted as shown in Figure 2.6.

By multiplying the output voltage and current, power of the solar cell can be calculated and a plot of power against voltage (P-U) obtained. It is also shown in Figure 2.6.

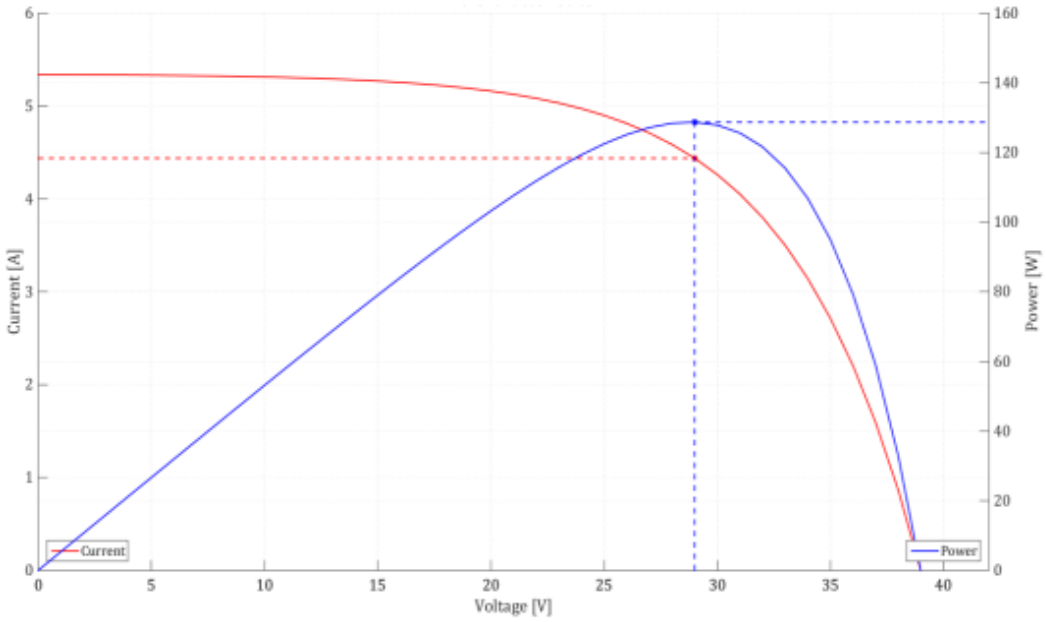

Figure 2.6: P-U and I-U Characteristics of a Solar PV Cell [6]

The power of the solar cell is the product of the current and voltage. It is the power that can be delivered to the external circuit. At a particular voltage and current point, the solar cell gives a maximum power. This point is termed the maximum power point (MPP) and is the most desirable point of operation. The point is shown at the intersection of the blue and red

lines in Figure 2.6. In terms of efficiency, most commercial solar cell has an efficiency of 15-20 percent (%) and means a large area would be needed for higher power values. Therefore, it is important at all times the solar cell is giving out maximum power. With reference to Figure 2.2, the dc-dc converter part of the system incorporates maximum power point tracking (MPPT) system. The MPPT ensures that at all times the solar cell is operating at the maximum power point.

2.1.3 Solar PV Cell Operation

The operation of a PV solar cell centers on the action of solar irradiation and movement of holes/electrons in the p-n region and junction of the semiconductor material. The sun gives the cell solar radiation, G, which results in a current according to equation (2.3). The variation of solar irradiation causes different output currents from the cell and a shift in the maximum power point for the cell. An increase in irradiation causes an increase in the current and a decrease results in the decrease of the current. This is because the current produced is direct proportional to solar irradiation. The behavior of the cell with different solar irradiance (G1, G2, G3 and G4) is shown in Figure 2.7.

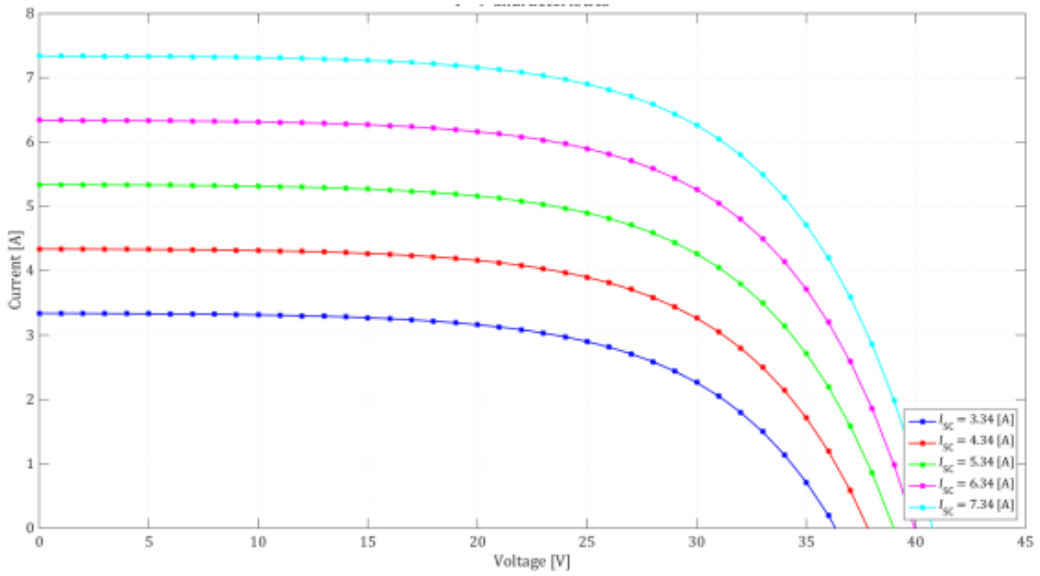

Figure 2.7: I-U Characteristics for Different radiation [6]

The characteristic I-U curves of Figure 2.7 show the change in current and voltage with varying solar irradiation. It can also be seen from Figure 2.7 that the change in irradiance causes a shift in the maximum power point of the cell.

Another parameter of interest is the solar cell temperature. The temperature increase has an impact on the voltage of the cell. As the temperature increases, the voltage reduces. This is mainly due to increasing internal carrier recombination rate as a result of higher carrier concentration with increasing temperature [12]. At a particular solar irradiation G, an increase in solar cell temperature results in a rapid decrease in power output.

The overall operation of a solar PV cell is affected by its efficiency, irradiance and temperature. These parameters cause changes to the power output of the cell and consequently the maximum power point (MPP).

2.2 PV Penetration

$$PV\ Penetration\ Level = \frac{PV\ Generated\ Capacity\ (kWh\ or\ MWh)}{Network\ Peak\ Load\ (kWh\ or\ MWh)}$$

2.3 Small Signal Stability

Small-signal stability analysis is about power system stability when subject to small disturbances. If power system oscillations caused by small disturbances can be suppressed, such that the deviations of system state variables remain small for a long time, the power system is stable. On the contrary, if the magnitude of oscillations continues to increase or sustain indefinitely, the power system is unstable. Power system small-signal stability is affected by many factors, including initial operation conditions, strength of electrical connections among components in the power system, characteristics of various control devices, etc. Since it is inevitable that power system operation is subject to small disturbances, any power system that is unstable in terms of small-signal stability cannot operate in practice. In other words, a power system that is able to operate

normally must first be stable in terms of small-signal stability. Hence, one of the principal tasks in power system analysis is to carry out small-signal stability analysis to assess the power system under the specified operating conditions.

Chapter 3

Mathematical Model of System

Figure 3.1 shows the configuration of a single-machine infinite bus power system, where a large-scale PV power generation plant is connected at busbar s. Typical voltage-current characteristic of PV generation is non-linear, given by the following expression [13].

$$V_{pv} = \frac{N_s nkT}{q} \ln\left(\frac{\frac{N_p I_{sc} I_r}{100} - I_{pv}}{N_p I_0} + 1 \right) \quad (1)$$

where **T** is the junction temperature, **Ir** the irradiance, **Ns** and **N p** number of cells in series and parallel respectively, **n** ideality factor, **k** Boltzmann's constant, **q** charge of the electron, **Isc** short-circuit current and **I**0 saturation current.

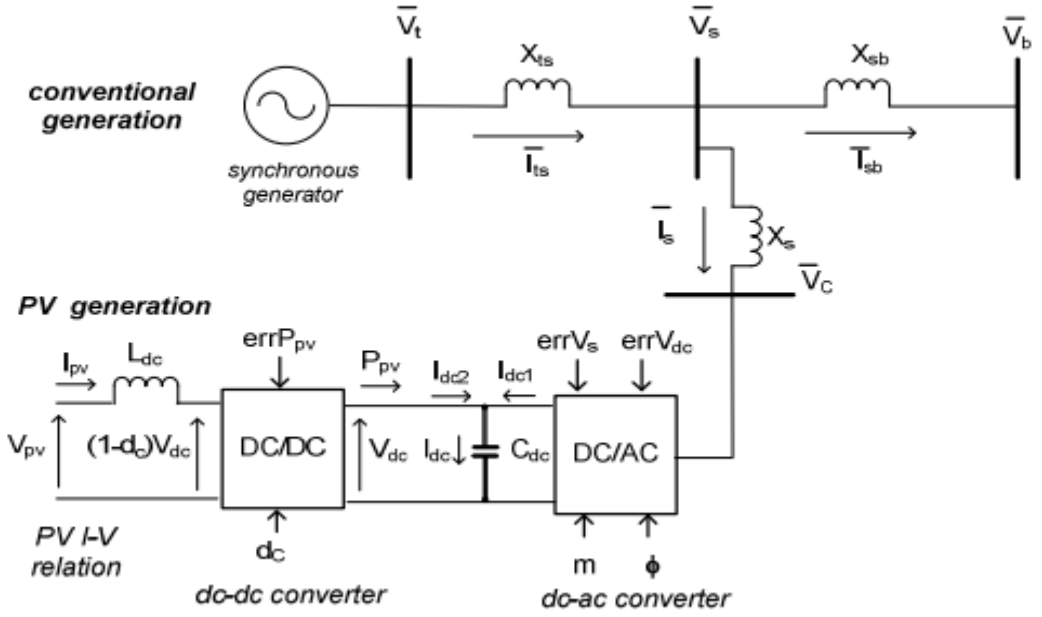

Figure 3.1: A power system integrated with a PV generation plan

In Figure 3.1, the PV power plant is connected to the power system through a two-stage topology of inverter system, which is usually employed by gird-connected PV generation [14][15]. In addition to the function of enhancing output DC voltage, DC/DC inverter is mainly for implementing the maximum power point tracking (MPPT) control. As illustrated by Figure 3.2, change of PV output current and voltage change are affected by variations of various factors, such as the irradiance, Ir . In order to make full use of PV cells (due to their limited life span and high initial cost), MPPT is employed in order to extract as much power from them as possible by controlling the cycle duty of the DC/DC inverter, dc. Design and implementation of MPPT control has been one of the most important issues in developing PV generation. Many methods have been proposed, such as the curve-fitting technique, perturb-and observe method, etc., considering the need of practical operation of PV generation [16]-[19]. Basically, the objective of MPPT is to ensure the operation of PV generation to be on the curve, Ppv-max , by controlling dc . Because in establishing the mathematical model of PV generation integrated with the power system of Figure 3.1, the purpose is to investigate the impact of PV generation on the power system by theoretical analysis, numerical computation and simulation (not experiment). Hence it must be

assumed that the characteristic of PV generation of Eq.(1) is given such that the curve **Ppv**-max can be obtained. Therefore, the function of MPPT can be modeled as,

$$d_c = d_{c0} + K_{pv}(s)(P_{pv} - P_{pv\max}) \quad (2)$$

no matter what scheme it is implemented in practice, where **K pv (s)** is the transfer function of the MPPT controller. Dynamic of the DC/DC inverter can be modeled simply to be

$$\dot{I}_{pv} = \frac{1}{L_{dc}}[V_{pv} - (1 - d_c)V_{dc}] \quad (3)$$

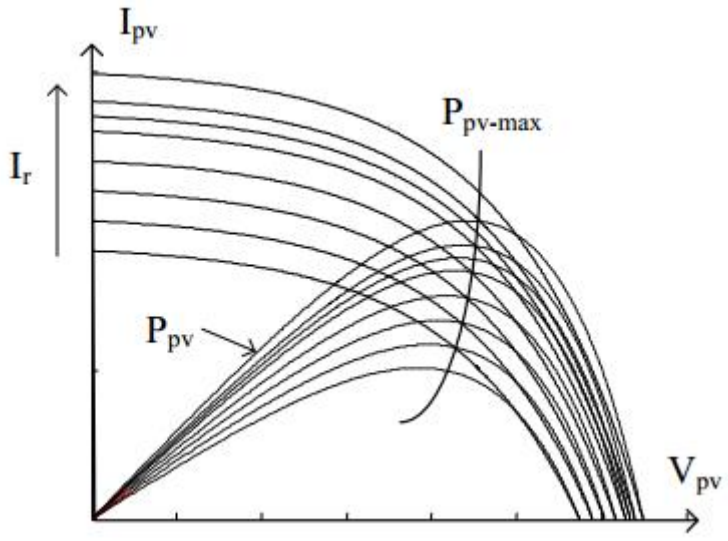

Figure 3.2: Non-linear V-I characteristic of PV generation

DC/AC inverter usually employs the PWM (pulse width modulation) control to regulate the exchange of active and reactive power between the PV generation and the rest of the power system. This can be achieved by controlling the modulation ratio **m** and phase **φ** of the PWM algorithm through the following AC and DC voltage control function respectively

$$m = m_0 + K_{ac}(s)(V_s - V_{sref})$$
$$\phi = \phi_0 + K_{dc}(s)(V_{dc} - V_{dcref}) \quad (4)\ \&\ (5)$$

Where **Kac (s)** and **Kdc (s)** is the transfer function of the ac and dc voltage controller respectively.

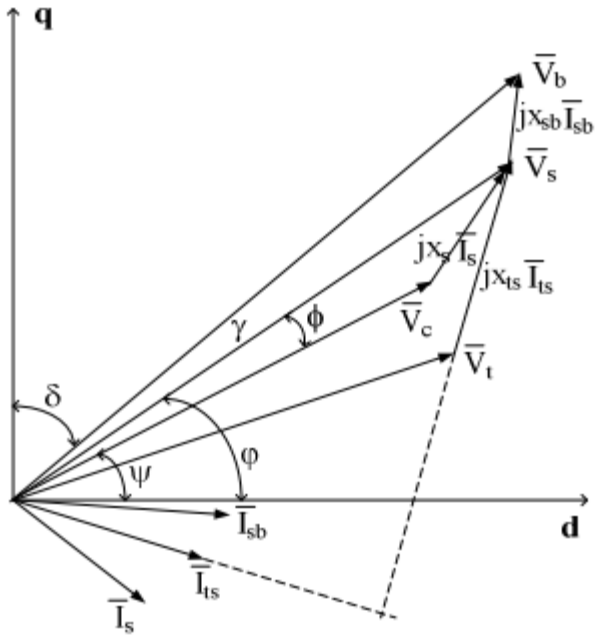

Figure 3.3: Phasor diagram of power system of Figure 3.1

AC voltage at terminal of the DC/AC inverter, **VC** , can be expressed in the **d-q** coordinate of the generator (Figure 3.3) to be [25]

$$\overline{V}_c = mkV_{dc}(\cos\psi + j\sin\psi) = mkV_{dc}\angle\psi \quad (6)$$

where k is the converter ratio dependent of inverter structure, V_{dc} is the DC voltage across the capacitor C_{dc}. Active power received by the DC/AC inverter from the power system is

$$V_{dc}I_{dc1} = i_{sd}v_{cd} + i_{sq}v_{cq} = i_{sd}mkV_{dc}\cos\psi + i_{sq}mkV_{dc}\sin\psi \quad (7)$$

where subscript d and q denotes the d and q component of the variable respectively. Hence

$$I_{dc1} = i_{sd} mk \cos\psi + i_{sq} mk \sin\psi \quad (8)$$

Because

$$P_{pv} = I_{pv} V_{pv} = I_{dc2} V_{dc} = (1 - d_c) V_{dc} I_{pv} \quad (9)$$

Hence $\boldsymbol{I_{dc2}} = (1\text{-}d_c)\, \boldsymbol{I_{pv}}$ such that dynamic of the DC/AC inverter is expressed to be

$$\dot{V}_{dc} = \frac{1}{C_{dc}} (I_{dc1} + I_{dc2})$$
$$= \frac{1}{C_{dc}} [i_{sd} mk \cos\psi + i_{sq} mk \sin\psi + (1 - d_c) I_{pv}] \quad (10)$$

General mathematical model of the synchronous generator can be written as **X g = F** (**Xg**, ***Its***), where **X g** is the state variable vector associated with generator dynamics and ***Its*** (or ***itsd*** and ***itsq***) is the interface variable between the generator and rest of the system. In this paper, the following generator model is used, which is sufficient for the study of power system small signal oscillation stability [22].

$$\dot{\delta} = \omega_o(\omega - 1)$$
$$\dot{\omega} = \frac{1}{M}[P_m - P_t - D(\omega - 1)]$$
$$\dot{E}_q' = \frac{1}{T_{d0}'}(-E_q + E_{fd})$$
$$E_{fd}' = TE(s)(V_{tref} - V_t) \qquad (11)$$

where for simplicity of discussion, transfer function of the AVR (automatic voltage regulator) is taken to be a first-order system $TE(s) = \frac{\mathrm{KA}}{1+\mathrm{sTA}}$ in this paper and

$$P_t = E_q' i_{tsq} + (x_q - x_d')i_{tsd} i_{tsq}$$
$$E_q = E_q' - (x_d - x_d')i_{tsd}$$
$$V_t = \sqrt{v_{td}^2 + v_{tq}^2} = \sqrt{(x_q i_{tsq})^2 + (E_q' - x_d' i_{tsd})^2} \qquad (12)$$

From figure 3.1 it can have

$$\bar{V}_t = jx_{ts}\bar{I}_{ts} + \bar{V}_s$$
$$\bar{V}_s = jx_s\bar{I}_s + \bar{V}_c$$
$$\bar{V}_s - \bar{V}_b = jx_{sb}(\bar{I}_{ts} - \bar{I}_s)$$

Those equations above give

$$jx_s\bar{I}_s + \bar{V}_c - \bar{V}_b = jx_{sb}(\bar{I}_{ts} - \bar{I}_s)$$
$$\bar{V}_t = jx_{ts}\bar{I}_{ts} + jx_{sb}(\bar{I}_{ts} - \bar{I}_s) + \bar{V}_b \qquad (13)$$

In d-q coordinate of the generator, as shown by Figure 3.3, from Eq.(13) it can be obtained that

$$\begin{bmatrix} x_{sb} & -x_s - x_{sb} \\ x_q + x_{ts} + x_{sb} & -x_{sb} \end{bmatrix} \begin{bmatrix} i_{tsq} \\ i_{sq} \end{bmatrix} = \begin{bmatrix} -V_c \cos\psi + V_b \sin\delta \\ V_b \sin\delta \end{bmatrix}$$
$$\begin{bmatrix} x_{sb} & -x_s - x_{sb} \\ x_d' + x_{ts} + x_{sb} & -x_{sb} \end{bmatrix} \begin{bmatrix} I_{tsd} \\ I_{sd} \end{bmatrix} = \begin{bmatrix} V_c \sin\psi - V_b \cos\delta \\ E_q' - V_b \cos\delta \end{bmatrix} \quad (14)$$

The complete mathematical model of the power system of Figure 3.1 thus is established, consisted of the model of PV generation and control of Eq.(1)-(5) and (9), generator of Eq.(10) and (11), and integration of the generator and the PV power plant with the rest of the power system of Eq.(14).

Chapter 4

Result

Parameters and initial operating conditions of an example single-machine infinite-bus power system integrated with a PV power plant of Figure 3.1 are given in Appendix. The effective technique of damping torque analysis (DTA) [22]- [24] was used to study the oscillation stability of the power system as affected by the PV power plant. Appendix I presents the details of deriving the linearized model of the power system integrated with the PV power plant of Figure 3.1, given by (A-2) and (A-8)-(A-11). Computational results of damping torque contribution from the PV power plant, confirmed by the computational results of system oscillation mode, from the complete linearized model of Figure 4 and 5 are given in Table 4.1 and 4.2. In Table 4.1, the total active power supplied by the generator and PV power plant to the load at the infinite busbar is fixed at 1.0 p.u., but level of mixture of conventional and PV power generation varies. In Table 4.2, the PV power generation is fixed to be 0.3 p.u., but active power supply from the generator changes.

Table 4.1: Computational results of the example power system when total active power received at the infinite busbar is fixed at 1.0 p.u. ($P_{t0} + P_{pv0} = 1.0$ p.u.)

P_{t0}	P_{pv0}	ψ_0 (degree)	ΔT_{dt}	ΔT_{ddt}	ΔT_{dt-ac}	Oscillation mode
1.0	0.0	54.3	1.80	1.43	0.0006	$-0.57 \pm j\ 3.86$
0.9	0.1	58.6	1.12	0.79	0.0015	$-0.43 \pm j\ 3.97$
0.8	0.2	62.9	0.49	0.21	0.0021	$-0.31 \pm j\ 4.09$
0.7	0.3	67.4	-0.09	-0.32	0.0023	$-0.22 \pm j\ 4.49$
0.6	0.4	72.1	-0.62	-0.81	0.0021	$-0.15 \pm j\ 4.29$
0.5	0.5	76.8	-1.11	-1.27	0.0017	$-0.09 \pm j\ 4.39$
0.4	0.6	81.5	-1.56	-1.68	0.0010	$-0.04 \pm j\ 4.47$
0.3	0.7	86.4	-1.97	-2.06	-0.0000	$0.01 \pm j\ 4.55$
0.2	0.8	91.3	-2.36	-2.42	-0.0012	$0.04 \pm j\ 4.62$
0.1	0.9	96.1	-2.72	-2.75	-0.0003	$0.07 \pm j\ 4.69$

Table 4.2: Computational results of the example power system when the PV power generation is fixed at 0.3 p.u. ($P_{pv0} = 0.3$ p.u.)

P_{t0}	ψ_0 (degree)	ΔT_{dt}	ΔT_{ddt}	ΔT_{dt-ac}	Oscillation mode
0.1	89.6	-2.04	-2.07	-0.0000	$-0.01 \pm j\ 8.13$
0.2	85.8	-1.75	-1.81	0.0001	$-0.06 \pm j\ 8.09$
0.3	81.9	-1.45	-1.55	0.0003	$-0.12 \pm j\ 8.05$
0.4	78.2	-1.14	-1.27	0.0006	$-0.17 \pm j\ 7.99$
0.5	74. 6	-0.81	-0.99	0.0010	$-0.23 \pm j\ 7.93$
0.6	70.9	-0.46	-0.67	0.0016	$-0.29 \pm j\ 7.85$
0.7	67.5	-0.09	-0.33	0.0023	$-0.36 \pm j\ 7.76$
0.8	64.1	0.33	0.05	0.0031	$-0.44 \pm j\ 7.64$
0.9	60.8	0.80	0.49	0.0042	$-0.52 \pm j\ 7.51$
1.0	57.6	1.34	0.97	0.0056	$-0.61 \pm j\ 7.35$

From Table 4.1 and 4.2 it can be seen that

1) Damping torque supplied by the PV power plant changes at different levels of mixture of conventional and PV power generation, which can be positive or negative. With the fixed load at the infinite busbar, the more power contributed by the PV generation, the worse the impact of PV generation on system oscillation stability, because the more negative damping torque is provided by the PV power plant.

2) Damping torque supplied by the PV power plant also changes from positive to negative at different levels of conventional power generation even though the PV power generation is fixed. In this case, the lighter the load of conventional power generation (power supplied by the generator), the worse the impact of the PV generation on power system oscillation stability.

3) Damping torque contribution from the PV power plant changes sign between ψ 0 = 62.90 and ψ_0 = 67.40 (Table 1) or ψ_0 = 64.10 and ψ_0 = 67.50 (Table 4.2). Hence there must exist a critical operating condition **ψ critical** when the damping torque contribution from the PV power plant changes sign. The operation of the PV power plant should avoid **$\psi_0 > \psi$ critical** when it provides negative damping to power system oscillation.

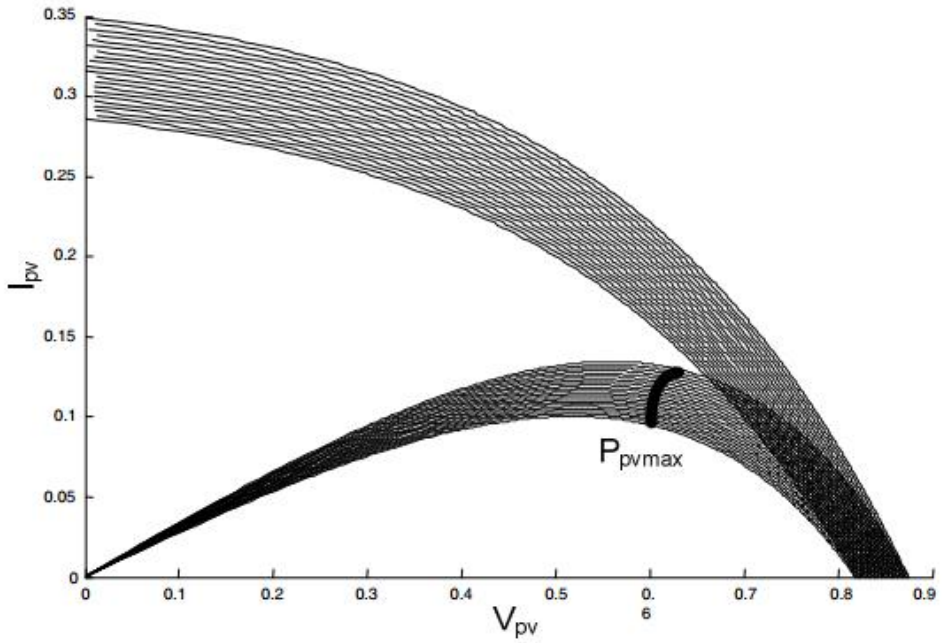

Figure 4.1: Set of simulated V-I characteristic of PV generation and tracking of the MPP

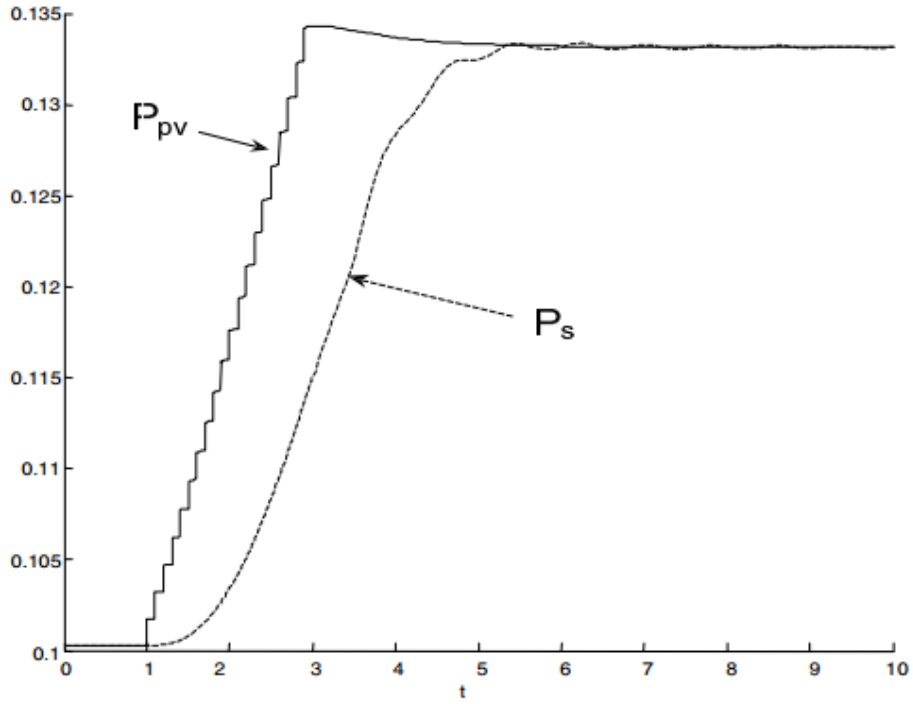

Figure 4.2: Power output from the DC/DC and DC/AC inverter of the PV power plant

Non-linear simulation using the non-linear model given in chapter 3 of the paper was carried out to verify the mathematical model and confirm the results of computation from system linearized model. Figure 4.1 and 4.2 shows the simulation results when the irradiance changed at 1.0 second of the simulation. The change was a step increase of 1% every 0.1 second and lasted for 2 seconds. Figure 4.1 shows the set of V-I curves of PV generation used and tracking of the maximum power point. Figure 4.2 is the power output from the DC/DC and DC/AC inverter of the PV power plant respectively.

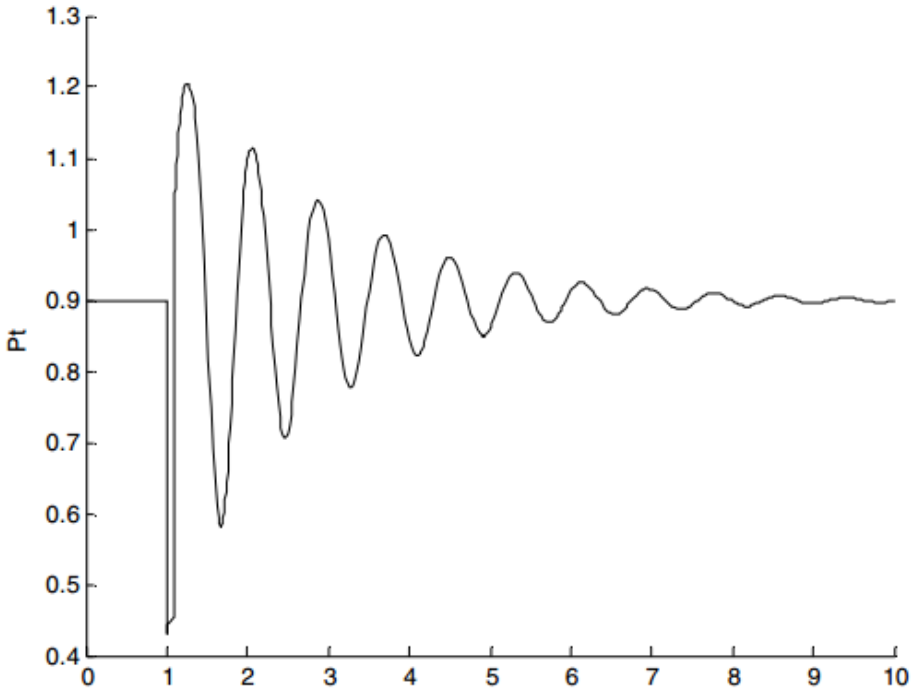

Figure 4.3: P_{to} = 0.9 p.u. and Ppv0 = 0.1 p. u.

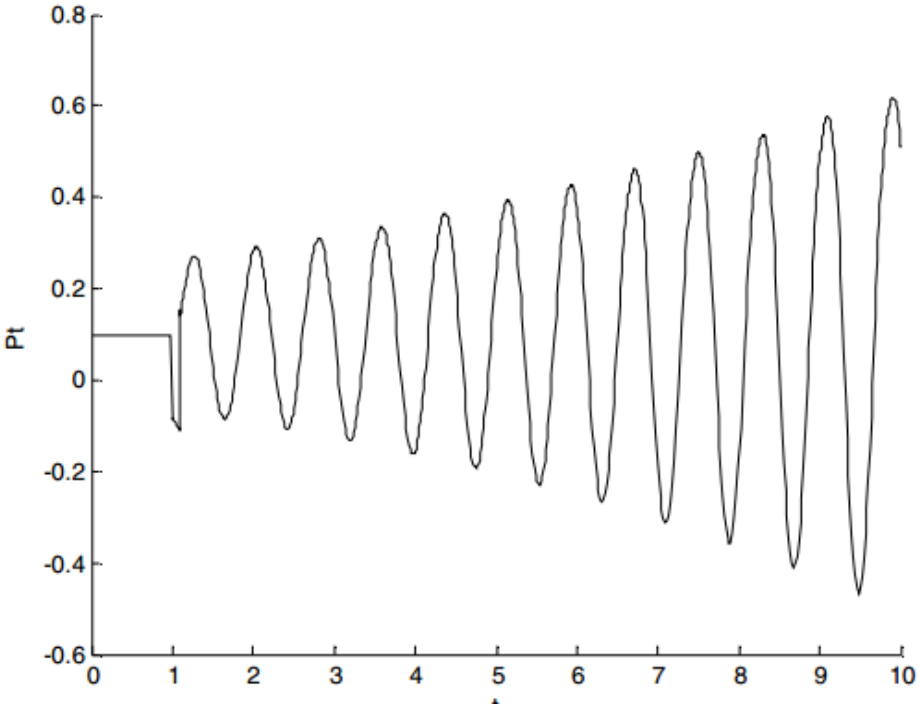

Figure 4.4: P_{to} = 0.1 p.u. and Ppv0 = 0.9 p. u.

Simulation at two different levels of mixture of conventional and PV power generation when the total power received by the load at the infinite busbar was fixed at 1.0 p.u.

Figure 4.3 and 4.4 gives the results of simulation (the fault applied was the three-phase to-earth short circuit on the transmission line occurred at 1 second of simulation for 100ms) at two different levels of mixture of conventional and PV power generation when the total power received by the load at the infinite busbar was fixed at 1.0 p.u. Figure 4.5 and 4.6 is the results of simulation at two different levels of conventional generation and the PV power generation was fixed at 0.3 p.u. Those results of non-linear simulation confirm both the analysis in the above section and computational results presented in Table 4.1 and 4.2.

1) When the total power received by the load is fixed, the heavier load condition the SOFC power plant operates at, the more it will damage the damping of power system oscillation;

2) When the SOFC power generation is fixed, the lighter the load condition of the conventional power plant is, the more negative damping torque is provided by the SOFC power plant.

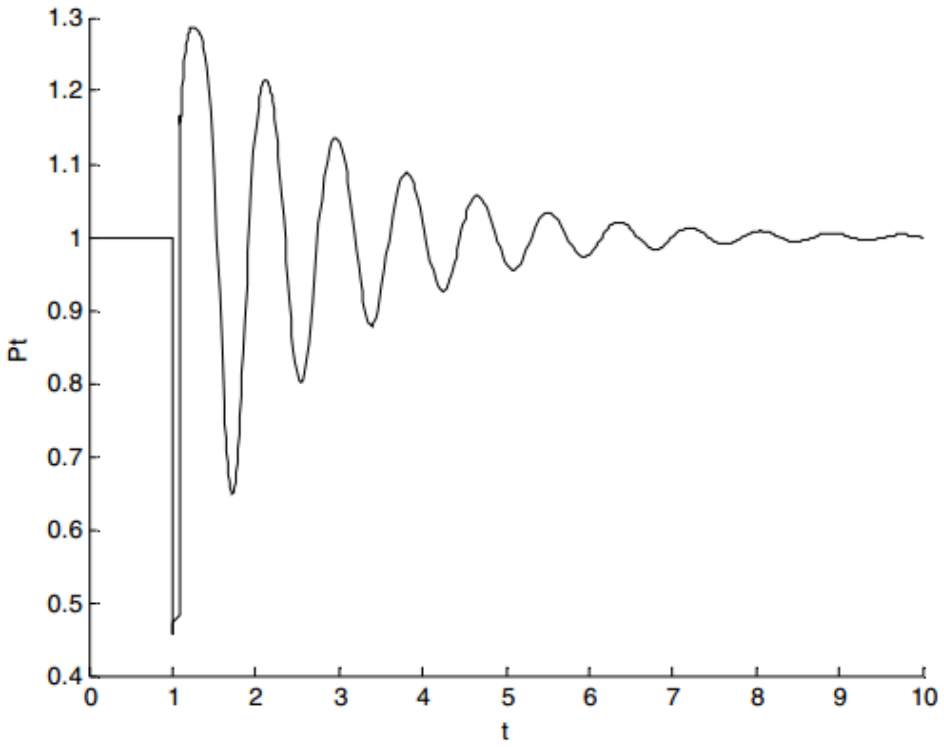

Figure 4.5: P_{to} = 1.0 p.u. and Ppv0 = 0.3 p. u.

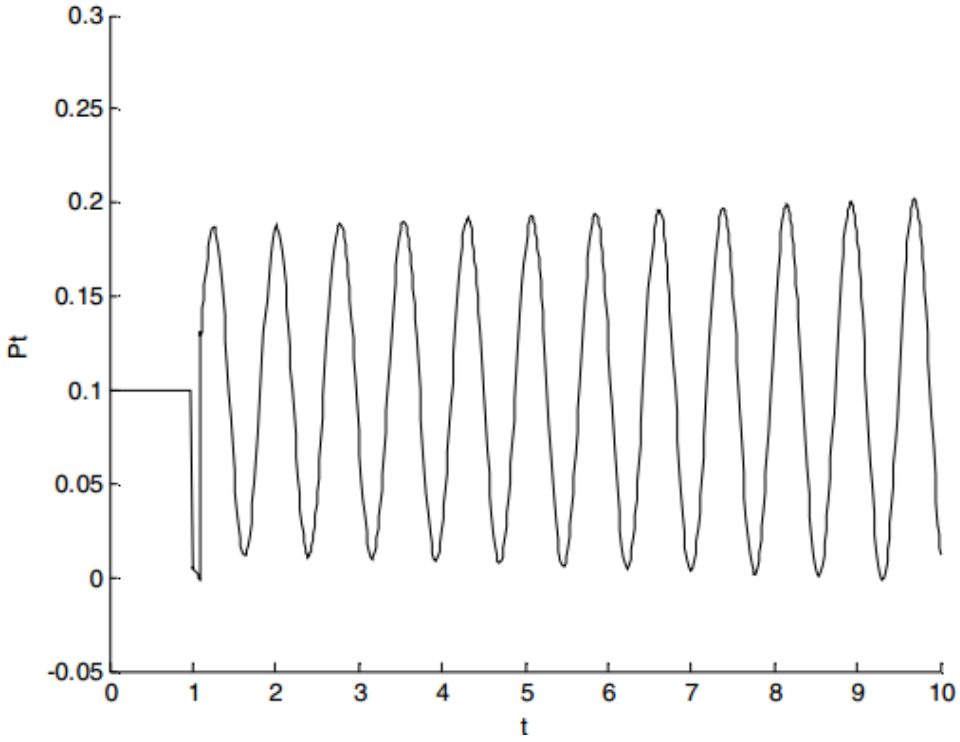

Figure 4.6: P_{to} = 0.1 p. u. and Ppv0 = 0.3 p. u.

Simulation when the generator operated at two loading conditions and the PV power generation was fixed at 0.3 p.u.

Chapter 5

Conclusion

The paper investigates the impact of grid-connected PV generation on power system small signal oscillation stability. Conventional technique of damping torque analysis is used for the investigation of a single-machine infinite-bus power system integrated with a PV power plant. Results of damping torque computation, confirmed by calculation of system oscillation mode and non-linear simulation, of an example power system integrated with a PV power plant are presented in the paper. They demonstrate that the effect of PV penetration on system oscillation stability varies with changes of system operating conditions, because the damping torque contribution from the PV generation can be positive or negative. The critical operating condition of the PV power plant is when its damping torque contribution changes sign, which in fact indicates a stability limit of PV operation as far as power system oscillation stability is concerned. The effect of PV generation on system oscillation stability is negative beyond the critical operating condition. When the total load is fixed, a higher PV penetration should be avoided because this increases the chance of its damaging system oscillation stability. When the PV penetration is fixed, its operation can also approach to the critical operating condition with the decrease of conventional power generation.

References

[1] J. Widen, E. Wäckelgård, J. Paatero and P. Lund, “Impacts of distributed photovoltaics on network voltages: Stochastic simulations of three Swedish low-voltage distribution grids,” *Electric power systems research,* vol. 80, pp. 1562-1571, 2010.

[2] P. Kundur, "Power System Stability and Control", New York: McGraw-Hill, Inc., 1994 Edition.

[3] T. V. Cutsem and C. Vournas, Voltage Stability of Electric Power Systems, Kluwer Academic Publishers, 1998.

[4] Y. Xue, M. Manjrekar, C. Lin, M. Tamayo and J. N. Niang, “Voltage Stability and Sensitivity Analysis of Grid-Connected Photovoltaic Systems,” in Power and Energy Society General Meeting, San Diego,CA, 2011.

[5] E. Pihl, “Concentrating Solar Power,” Energy Committee of Royal Swedish Academy of Sciences, Stockholm, 2009.

[6] M. Bollen och H. Fainan, "Integration of Distributed Generation in the Power System", Hoboken, New Jersey: John Wiley and Sons, Inc, 2011.

[7] Lecture no.8 in, “SPPT (part 1 and 2),” Chalmers University of Technology, 2014

[8] R. A. Shalwala, “PV Integration into Distribution Networks in Saudi Arabia”, PhD Thesis, University of Leicester, Leicester, 2012.

[9] R. Boylestad and L. Nashelsky, "Electronic Devices and Circuit Theory", New Jersey: Pearson Prentice Hall, 2009.

[10] K. Giannouloudis and E. Mulenga, “PV Systems and Applications,” ENM-095: Sustainable Power Production and Transportation Scientific Paper, Gothenburg, 2014.

[11] C. R. Nave, “The P-N Junction,” Physics World, 2012. [Online]. Available: http://hyperphysics.phy-astr.gsu.edu/hbase/solids/pnjun.html#c3.[Accessed 20 September 2014].

[12] S. Dubey, J. N. Sarvaiya and B. Seshadri, “Temperature Dependent Photovoltaic (PV) Efficiency and Its Effect on PV Production in the World,” Energy Proceedings, vol. 33, no. 1, pp. 331-321, 2012.

[13] Y. T. Tan, D. S. Kirschen and N. Jenkins, “A model of PV generation suitable for stability analysis”, IEEE Trans. on Energy Conversion, Vol.19, No.4, 2004, pp748-755

[14] J. M. Carrasco, L. G. Franquelo, etc., “Power electronic systems for the grid integration of renewable energy sources: a survey”, IEEE Trans. On Industrial Electronics, Vol. 53, No.4, 2006, pp1002-1016

[15] S. B. Kjaer, J. K. Pedersen and F. Blaabjerg, “A review of single-phase grid-connected inverters for photovoltaic modules”, IEEE Trans. on Industry Applications, Vol. 41, No.5, 2005, pp1292-1306

[16] S. Jain and V. Agarwal, “A single-stage grid connected inverter topology for solar PV systems with maximum power point tracking”, IEEE Trans. On Power Electronics, Vol. 22, No. 5 2007, pp1928-1940

[17] K. K. Tse, M. T. Ho, H. S. H. Chung and S. Y. Hui, “A novel maximum power point tracker for PV panels using switching frequency modulation”, IEEE Trans. on Power Electronics, Vol. 17, No.6, 2002, pp980-989

[18] S. Jain and V. Agarwal, “Comparison of the performance of maximum power point tracking schemes applied to single-phase grid-connected photovoltaic systems”, IET Proc. Electric Power Applications, Vol.5, No.1, 2007, pp753-762

[19] M. T. Ho and H. S. H. Chung, “An integrated inverter with maximum power tracking for grid-connected PV systems”, IEEE Trans. on Power Electronics, Vol. 20, No.4, 2005, pp953-962

[20] L. Wang and T. Lin, “Dynamic stability and transient responses of multiple grid-connected PV systems”, Proc. of IEEE PES T&D Conference, 2008, pp1-8

[21] Y. T. Tan and D. S. Kirschen, “Impact on the power system of a large penetration of photovoltaic generation”, Proc. of IEEE PES General Meeting, 2007, pp1-8

[22] Y. N. Yu, Electric Power System Dynamics, Academic Press Inc., 1983 [11] F. P. deMello and C. Concordia, “Concepts of synchronous machine stability as affected by excitation control”, IEEE Trans. Power Appar. Syst., Vol.88, No. 4, 1969 pp316-329

[23] E.V. Larsen and D.A. Swann, “Applying power system stabilizers Part IIII”, IEEE Trans. Power Appar. Syst., Vol. 100, No. 6, 1981, pp3017-3046

[24] “Modeling of power electronics equipment (FACTS) in load flow and stability programs”, CIGRE T F 38-01-08, 1998

[25] W.G.Heffron and R.A.Phillips, “Effect of a modem amplidyne voltage regulator on under excited operation of large turbine generator”, AIEE Trans. 71, 1952

[26] H .F. Wang, “Phillips-Heffron model of power systems installed with STATCOM and applications”, IEE Proc. Part C, Vol.146, No.5, 1999, pp521- 527

[27] H.F.Wang and F.J.Swift, ‘The capability of the Static Var Compensator in damping power system oscillations’, IEE Proc. Part C, May, No.4, 1996

Appendix

Transmission line: $x_{ts} = 0.2 p.u., x_{sb} = 0.2 p.u., x_s = 0.2 p.u.$;

Generator:

$x_d = 1.3 p.u., x_q = 0.47 p.u., x'_d = 0.3 p.u., M = 3s., D = 2 p.u., T'_{d0} = 5s.$;

AVR: $T_A = 0.1s. K_A = 10 p.u.$;

Initial load condition: $V_{t0} = 1.0 p.u., V_{s0} = 1.0 p.u., V_{b0} = 1.0 p.u.$

PV power plant:

For the simplicity of analysis, it is assumed that control functions of PV generation are implemented by proportional control law. Hence linearization of Eq.(2), (4) and (5) is

$$\Delta d_c = K_{pv} \Delta P_{pv}, \Delta m = K_{ac} \Delta V_s, \Delta \phi = K_{dc} \Delta V_{dc} \quad \text{(A-1)}$$

From Figure 3 it can be seen that $\Delta \psi = -\Delta \phi$. Hence it can have

$$\Delta \psi = K_{dc} \Delta V_{dc} \quad \text{(A-2)}$$

Linearization of Eq.(1) and (8) is

$$\begin{aligned} \Delta V_{pv} &= a_1 \Delta I_{pv}, \\ \Delta P_{pv} &= V_{pv0} \Delta I_{pv} + I_{pv0} \Delta V_{pv} = a_2 \Delta I_{pv} \end{aligned} \quad \text{(A-3)}$$

That gives

$$\Delta d_c = K_{pv} a_2 \Delta I_{pv} \quad \text{(A-4)}$$

Because $\bar{V}_s = jx_s\bar{I}_s + \bar{V}_c, V_s = \sqrt{v_{sd}{}^2 + v_{sq}{}^2}$, it can have

$$v_{sd} = -x_s i_{sq} + kmV_{dc}\cos\psi, v_{sq} = x_s i_{sd} + kmV_{dc}\sin\psi$$

Hence

$$\Delta V_s = b_1\Delta\delta + b_2\Delta E_q' + b_3\Delta V_{dc} + b_4\Delta m + b_5\Delta\psi \quad \text{(A-5)}$$

From Eq.(A-1), (A-2) and (A-5) it can have

$$\Delta m = \frac{K_{ac}}{1 - b_4 K_{ac}}(B_6\Delta\delta + B_7\Delta E_q' + B_8\Delta V_{dc}) \quad \text{(A-6)}$$

By using Eq.(A-2) and (A-6), linearization of Eq.(14) can be obtained to be

$$\begin{bmatrix}\Delta i_{tsd}\\ \Delta i_{tsq}\\ \Delta i_{sd}\\ \Delta i_{sq}\end{bmatrix} = \mathbf{C}\begin{bmatrix}\Delta\delta\\ \Delta E_q'\\ \Delta V_{dc}\\ \Delta\psi\\ \Delta m\end{bmatrix} = \begin{bmatrix}c_{11} & c_{12} & c_{13}\\ c_{21} & c_{22} & c_{23}\\ c_{31} & c_{32} & c_{33}\end{bmatrix}\begin{bmatrix}\Delta\delta\\ \Delta E_q'\\ \Delta V_{dc}\end{bmatrix} \quad \text{(A-7)}$$

Linearization of Eq.(3) and (9) is

$$\Delta\dot{I}_{pv} = C_1\Delta I_{pv} + C_2\Delta V_{dc} \quad \text{(A-8)}$$

$$\Delta\dot{V}_{dc} = C_3\Delta\delta + C_4\Delta E_q' + C_5\Delta V_{dc} + C_6\Delta I_{pv} + K_{dm}\Delta m + K_{d\psi}\Delta\psi \quad \text{(A-9)}$$

Linearization of Eq.(10) is

$$\Delta\dot{\delta} = \omega_o\Delta\omega$$

$$\Delta\dot{\omega} = \frac{1}{M}(-\Delta P_t - D\Delta\omega)$$

$$\Delta\dot{E}_q' = \frac{1}{T_{d0}'}(-\Delta E_q + \Delta E_{fd}')$$

$$\Delta E_{fd}' = TE(s)(-\Delta V_t) \quad \text{(A-10)}$$

By using Eq.(A-2), linearization of Eq.(11) can be obtained to be

$$\Delta P_t = K_1\Delta\delta + K_2\Delta E_q' + (K_{pdc} + K_{p\psi}K_{vdc})\Delta V_{dc} + K_{pm}\Delta m$$

$$\Delta E_q = K_4\Delta\delta + K_3\Delta E_q' + (K_{qdc} + K_{q\psi}K_{vdc})\Delta V_{dc} + K_{qm}\Delta m \quad \text{(A-11)}$$

$$\Delta V_t = K_5\Delta\delta + K_6\Delta E_q' + (K_{vdc} + K_{v\psi}K_{vdc})\Delta V_{dc} + K_{vm}\Delta m$$

$$L_{dc} = 1.5\,p.u., C_{dc} = 1.0\,p.u., V_{dc0} = 1.0\,p.u., K_{dc} = 0.3, K_{ac} = 0.1, K_{pv} = 5$$